Supplemental Methods

Before fully developing the condition-specific models of *S.* Typhimurium in LB and LPM, numerical issues were addressed to ensure computational precision. The cplex solver from the IBM ILOG CPLEX Optimization Studio 12.4 was used in conjunction with a Python implementation of the COBRA toolbox.[1] To select a numerical tolerance for the solver, an iterative method was employed. Flux balance analysis[2] was used, selecting each model reaction in turn as an optimization objective to maximize. Iterative optimization identified 10^{-8} as a suitable numerical tolerance for distinguishing reactions that could carry flux from those that could not. The reactions that could carry flux in a given media were termed "accessible" in the media.

Next, model genes and metabolites were paired with omics data. Model genes matched directly to 1,251 probes, giving 98.5% coverage of 1,270 model genes. This left 19 model genes unpaired with the microarray. In order to match model metabolites, KEGG[3, 4] compound identifiers were assigned to identified metabolites. We were able to match 59 of 65 metabolites identified in LB culture and 59 of 64 metabolites identified in LPM culture to the model (Table SMT1).

Before building the fully omics-informed, constrained models, the ability to produce detected metabolites was investigated. As will be fully described elsewhere (Schmidt et al., in preparation), the Gene Inactivation Moderated by Metabolism, Metabolomics, and Expression (GIMMME) algorithm converts reversible reactions into two irreversible reactions, and further incorporates integer (binary) variables to ensure only one direction is used. "Virtual" metabolites are then added: e.g. each reaction that produces or consumes a real metabolite produces a virtual metabolite. A "virtual" metabolite reaction sink is then added, which makes it possible to precisely model the rate of production and consumption (turnover) of each model metabolite. Additionally, to ensure detected metabolites are produced and consumed by the metabolic network, it is possible to impose a requirement for a minimum reaction flux on the "virtual" metabolite reaction sink. By applying this constraint, we identified two experimentally detected metabolites that were present but could not be both produced and consumed (e.g. these metabolites were blocked) in each growth condition.

We then characterized the tradeoff between fully optimal growth and ensuring that the experimentally-detected metabolites were produced and consumed. Most, but not all, of the 57 metabolites in each condition that mapped to the model were accessible when growth was constrained to 100% of optimal. Each of the 57 could sustain flux (accessible) with relaxation of the growth constraints to 99% of optimal (Supplemental Methods Figure SMF1A). The tradeoff between growth and requiring metabolite production and consumption (turnover) was further verified. By requiring turnover at 1.01 times the numerical tolerance (1.01×10^{-8}) through all experimentally detected metabolites, reductions in maximal growth were smaller than the numerical tolerance (Supplemental Methods Figure SMF1B, LB Exp and LPM Exp.). Additionally, growth could still be achieved at greater than 99% of the optimal rate. By requiring turnover through all accessible metabolites, reductions in maximal growth in LPM were larger than the numerical tolerance (Supplemental Methods Figure SMF1B, LPM Acc.).

We then added "soft" penalties to the model reactions based on the transcriptomics measurements. Quantile-normalized intensities were taken from the two-color microarrays. Gene-reaction relations in the model were used to assign effective array intensities to the corresponding reactions. Flux through reactions incurred a penalty proportional to the difference in the normalized $\log_2$ intensity from the model locus with the highest intensity on the array. Since growth was constrained to 99% of optimal, the penalty was constrained to within 1% of the minimal achievable at the optimal growth rate. Therefore, fully condition-specific models comparing LB to LPM 4 h constrained growth to 99% of optimal, required flux through the experimentally-detected metabolites, and additionally constrained the transcriptome-derived penalty to within 1% of the minimal.

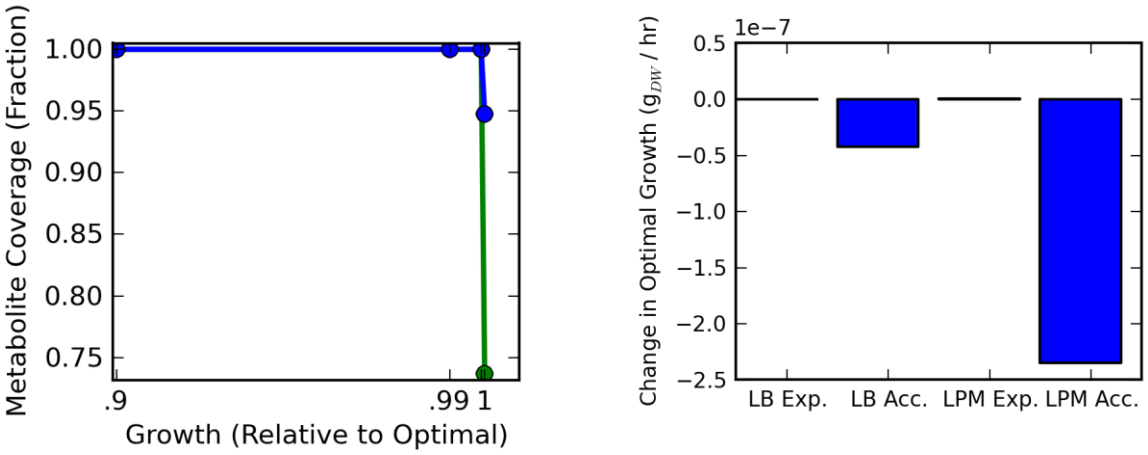

Supplemental Methods Figure SMF1. Numerical consistency check for imposition of "virtual" metabolite constraints. A) *S.* Typhimurium could utilize each of the 57 unblocked, experimentally detected metabolites represented in the model with growth constrained to 99% and 99.9% of the optimal rate, but not with growth constrained to 100% of the optimal rate. B) Imposition of flux constraints on all accessible metabolites resulted in a small relative reduction in the maximal achievable growth of less than 10^{-6}. Growth rate (biomass production) differences from the unconstrained model are shown. Constraints were imposed to ensure flux through LB experimentally detected metabolites (LB Exp.), all LB accessible metabolites (LB Acc.), LPM experimentally detected metabolites (LPM Exp.), and all LPM accessible metabolites (LPM Acc.).

We characterized the accessibility and essentiality of network reactions, cellular metabolites, and genes when either a requirement for non-zero growth or requirements for the more stringent conditions of near optimal growth, utilization of experimentally-detected metabolites, and near-minimal penalty were implemented (Supplemental Methods Table SMT2). The essentiality and accessibility of model reactions were also assessed for growth in LB and LPM media. A reaction was deemed essential if growth was no longer possible (i.e. zero growth or an "infeasible" solution) when the flux through the reaction was constrained to zero. As described previously, reactions were deemed to be accessible if their maximum flux, as assessed by flux balance analysis, was greater than the numerical tolerance for a given growth condition. Expanding the definition of essentiality to the growth- and omics-constrained models, a reaction was defined to be essential if it was no longer possible to meet the increased growth constraint as well as the metabolomics and transcriptomics data-derived constraints when fixing the reaction flux to zero. Gene and metabolite essentiality, as well as metabolite accessibility, were similarly assessed.

For comparison, the percentage of essential periplasmic and cytosolic metabolites surpassed the percentage of essential reactions in *S.* Typhimurium (e.g. 24.2% vs. 11.5% in LB, 28.7% vs. 15.1% in LPM, Supplemental Methods Table SMT2), consistent with a previous analysis of *E. coli* metabolism that employed flux-sum analysis.[5] In a previous investigation of essential metabolites for several bacteria cultured *in silico* with rich medium,[6] the intracellular pathogen *Mycobacterium tuberculosis* exhibited the largest number of essential metabolites, 358 (43%), compared with *E. coli* (128, 20%), *Staphylococcus aureus* (201, 35%), and *Helicobacter pylori* (139, 29%). Our result for *S.* Typhimurium (325 or 29% biochemically unique metabolites for minimal growth in LB medium) does raise the question as to whether metabolite essentiality may correlate with the degree to which a bacterium exhibits the capacity for a pathogenic lifestyle and its chosen environment. The metabolomics-driven systems biology approach employed herein may assist in the identification of new therapeutic targets. However, without a direct comparison to the host,[6, 7] it is not clear that increased essentiality enhances the availability of suitable drug targets. An integrated host-pathogen network that also monitors the capacity for macrophage activation may identify additional drug targets against intracellular pathogens by modulating host activation or the capacity of the host to supply essential microbial nutrients to the appropriate cellular compartment

Supplemental Methods Table SMT1: Reaction, gene, and metabolite accessibility and essentiality

	Model	LB (growth)		LB (near optimal growth + omics)		LPM (growth)		LPM (near optimal growth + omics)	
Network Reactions (essential)	2201	253	11.5%	386	17.5%	332	15.1%	391	17.8%
Network Reactions (accessible)	2201	1517	68.9%	1517	68.9%	1483	67.4%	1483	67.4%
Genes (essential)	1270	144	11.3%	230	18.1%	198	15.6%	260	20.5%
Cellular Metabolites, compartmentalized (essential)	1461	353	24.2%	456	31.2%	420	28.7%	472	32.3%
Cellular Metabolites, compartmentalized (accessible)	1461	985	67.4%	985	67.4%	971	66.5%	971	66.5%
Cellular Metabolites, biochemically unique (essential)	1114	325	29.2%	392	35.2%	390	35.0%	434	39.0%
Cellular Metabolites, biochemically unique (accessible)	1114	779	69.9%	779	69.9%	777	69.7%	777	69.7%

References

1. J. Schellenberger, R. Que, R. M. Fleming, I. Thiele, J. D. Orth, A. M. Feist, D. C. Zielinski, A. Bordbar, N. E. Lewis, S. Rahmanian, J. Kang, D. R. Hyduke and B. O. Palsson, *Nat Protoc*, 2011, **6**, 1290-1307.
2. J. D. Orth, I. Thiele and B. O. Palsson, *Nat Biotechnol*, 2010, **28**, 245-248.
3. M. Kanehisa and S. Goto, *Nucleic Acids Res*, 2000, **28**, 27-30.
4. M. Kanehisa, S. Goto, Y. Sato, M. Furumichi and M. Tanabe, *Nucleic Acids Res*, 2012, **40**, D109-114.
5. B. K. Chung and D. Y. Lee, *BMC Syst Biol*, 2009, **3**, 117.
6. T. Y. Kim, H. U. Kim and S. Y. Lee, *Metab Eng*, 2010, **12**, 105-111.
7. A. Navid, *Brief Funct Genomics*, 2011, **10**, 354-364.